

INFLUENCE OF GLASSY BACKBONE ON THE PHOTOFORMATION AND PROPERTIES OF SOLID ELECTROLYTES Ag : As-S-Ge

D. TSIULYANU*, I. STRATAN, M. CIOBANU

Department of Physics, Technical University of Moldova, bd. Dacia 41, Chisinau 2060, Moldova

The effect of the glassy backbone on the process of fabrication and some properties of solid electrolytes obtained via photodissolution (PD) of Ag into chalcogenide glasses (ChG) of the system As-S-Ge have been studied with respect to XRD and far IR spectroscopy analyses. The compositional tie – line $(\text{GeS}_4)_x(\text{AsS}_3)_{1-x}$ has been chosen to realize the monotonic transition of the structural units of glassy backbone from trigonal to tetragonal configuration. It is shown that the process of solid electrolyte formation occurs in three steps, but the last two steps, as well as the electrical properties of the finally fabricated electrolyte, are strongly influenced by chemical composition and microstructure of the used ChG backbone. The rate of solid electrolyte formation exhibit a maximum around of glassy backbone composition $(\text{GeS}_4)_{0.33}(\text{AsS}_3)_{0.67}$ but the electrical resistivity of fabricated solid electrolytes reaches a minimum at this composition. Based on IR transmission spectra analyses, it is assumed that these peculiarities are due to glass homogenization, which results from building in this alloyed composition of an amalgamation of tetrahedral and trigonal structural units connected in a random network, without clustering. Such homogenization promotes the transport of both electrons and ions involved in photoreaction because of lack of phase boundaries and additional defects.

(Received September 30, 2019; Accepted January 4, 2020)

Keywords: Glassy backbone, Solid electrolytes, Ag: As-S-Ge, IR measurements

1. Introduction

In the last decade glassy chalcogenides have become attractive for application in nonvolatile memory elements [1, 2] due to possibility of realization of an ionic charge transport and its transition to a metallic one. Ion transport is manifested at doping ChG with metals, such as Ag, Cu, Zn, with concentrations of the atoms of these metals exceeding a certain doping threshold. The concentration doping threshold depends on both ChG composition and used metal, but for Ag: GeS mixture it is established to be of about 6-8 at % [3]. At doping with higher concentrations of Ag, a dramatic intensification of ionic transport by up to 5-10 orders of magnitude occurs. Resulting glass materials exhibit a high ionic conductivity and therefore are called solid electrolytes or superionic chalcogenides. Superionic solid electrolytes can be fabricated via usual chemical synthesis of Ag based ChG [4], thermodiffusion or photodissolution (PD) of Ag into ChG. PD phenomenon has been discovered at the early stage of researches of chalcogenide glassy semiconductors [5] but still remains the most interesting and applicable due to the simple of both technology of fabrication and monitoring of solid electrolyte formation. The last can be realized using the measurement of the either electrical resistance [6] or optical transmittance [7] of the silver film as photodissolution proceeds. Kinetics of the solid electrolytes formation by photodissolution of Ag into GhG, apart from an induction period, usually consists of one or two linear steps followed by a parabolic tail [7] ascribed respectively to ion conductivity, photoconductivity and diffusion controlled process [8]. These processes strongly depend on temperature, incident light and parameters of two-layer structure ChG/ Ag, including the glass composition. In the present work we have focused our attention to effect of glassy backbone on

* Corresponding author: tsiudima@gmail.com

photoformation of Ag / ChG solid electrolyte, taking into consideration the percolation transitions in glassy random networks. For this purpose, the compositional tie – line $(\text{GeS}_4)_x (\text{AsS}_3)_{1-x}$ of the ternary As-S-Ge system has been chosen.

2. Materials and methods

The glassy alloys were prepared by melt-quenching method of pure (99, 99%) As, S and Ge, in quartz ampoules evacuated up to $5 \cdot 10^{-5}$ Torr. The ampoule was rotated around the longitudinal axis at velocity of 7-8 rotations / min and was agitated for homogenization during the synthesis time (24 h). The mixture was melted at 700-1000 °C depending on the composition. The ampoules were then quenched in air. Ampoules containing germanium-enriched alloys were quenched on a copper refrigerator with running water. The chemical compositions of synthesized materials are listed in Table 1 in the form of $(\text{GeS}_4)_x (\text{AsS}_3)_{1-x}$, which is the tie – line in the ternary As-S-Ge system. Additionally, to facilitate the IR spectra analyze have been synthesized GeS_2 and As_2S_3 . The ingots were clear and homogeneous but exhibited the glassy breaking edges. The glassy state of the synthesized materials was also confirmed by XRD analyses. The infrared transmission spectra have been registered in the far-infrared region (400 - 60cm^{-1}) with a Hitachi FIS-3 spectrophotometer, using powdered samples.

The chalcogenide thin films have been prepared by thermal “flash” evaporation of priority-synthesized materials onto Pyrex glass substrates, at room temperature. The evaporation was performed from a tantalum boat at the working pressure of 10^{-4} Pa. The area and the thickness of the grown chalcogenide films, determined using the optical microinterferometer MII – 4, were around $1,5 \text{ cm}^2$ and $1\mu\text{m}$ respectively. The silver films were deposited also by thermal evaporation in vacuum on top of the chalcogenide films, immediately (breaking the vacuum) after their preparation. The thickness of the silver film (controlled by equivalent quantity of evaporated Ag) was kept constant of about 50 nm.

Table 1. Composition and concentration of structural units of $(\text{GeS}_4)_x(\text{AsS}_3)_{1-x}$ glasses.

Nr.	Composition, [x]	Concentration, $\text{mol}/\text{cm}^3 \cdot 10^{-2}$		
		[AsS] _{3/2}	[GeS] _{4/2}	[SS] _{2/2}
1	0	1.57	0	1.17
2	0.17	1.30	0.26	1.23
3	0.33	0.96	0.48	1.2
4	0.5	0.69	0.69	1.21
5	0.67	0.44	0.88	1.23
6	0.83	0.22	1.08	1.24
7	1.00	0	1.22	—

The PD of silver onto ChG was performed by exposure the multilayer functional structure from the side of transparent substrate using the light of a 100W halogen lamp focused by a quartz lens. (Fig.1a).The incident power was measured by vacuum thermo element VTh-8 (Carl Zeiss, Germany) and was estimated at the sample surface as $\sim 250 \text{ mW}/\text{cm}^2$. The rate of solid electrolyte photoformation was measured by monitoring the changes that occur in the transmittance of the sample of broadband probing light with $\lambda = 650\text{-}3000 \text{ nm}$ that is in the range of whole transparency of studied ChG, as photodissolution proceeds. For this purpose the cut filter KC-15 was placed behind the sample, i.e. in front of photomultiplier, which served as light detector. A PC with a data acquisition board manufactured by National Instruments Inc. was used for processing. The electrical resistance of the thin film solid electrolytes has been measured at voltages much smaller than threshold voltage (off state), at which the ionic conductivity of solid electrolyte goes

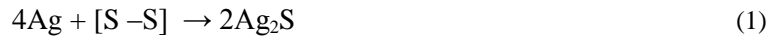
to metal conductivity, due to formation of a nanometric metallic electrodeposit [9, 10]. All measurements were carried out at room temperature.

3. Results and discussion

Fig. 1a shows schematically the multilayer structure of the sample. There are three well-defined boundaries: 1) substrate / undoped ChG; 2) undoped ChG / photodoped material (solid electrolyte); 3) photodoped material / Ag. During the photodissolution the boundary between photodoped material and undoped ChG propagates towards the substrate, but the boundary between photodoped material and Ag propagates in opposite direction i.e. towards surface, so that the thickness of both Ag layer and undoped ChG glass decrease with time. The rate of photodissolution of Ag, i.e. the rate of photoformation of the solid electrolyte was estimated by measuring the recovery rate of optical transmission of two-layer structure ChG / Ag in IR region of spectrum using a priori known dependence of Ag film transmittance on its thickness[11].

Figure 1b shows the unreacted Ag layer thickness versus exposure time for three (in order not to overload the picture) compositions of $(\text{GeS}_4)_x(\text{AsS}_3)_{1-x}$ system. For all compositions three stages of PD kinetics can be distinguished clearly: (I) the first, very sharp step is nearly independent on composition (except of GeS_4) but the thickness of Ag layer linearly decreases with exposure time, (II) the second one is a linear shoulder with a slope strongly influenced by ChG composition and the final (III) step, which reveals a dual behaviour: the thickness of Ag film, being plotted either versus exposure time or square-root of exposure time, shows a near linear dependence. We assert that the reason for such behaviour is the high speed of PD, making the process to occur on the beginning of parabolic curve, which is nearly a line.

Such behavior can be explained in terms of the mechanism based on a solid state reaction between Ag and ChG, which occurs simultaneously in two different spatial regions of the sample. At the first stage, the formation of a superionic conductor that is an Ag: ChG alloy with high ($10^{-5} - 10^{-3} \text{ Ohm}^{-1}\text{cm}^{-1}$) ionic conductivity at the interface occurs during deposition via chemical reaction between S-S segments and neutral Ag as [12]:



The existence of S-S segments in $(\text{GeS}_4)_x(\text{AsS}_3)_{1-x}$ alloys has been predicted already at early stage of investigation of these materials, which were treated [13] as an amalgamation of elemental structural units (s.u.) connected in a random network or comprising clusters of a scale of 10-20 Å.

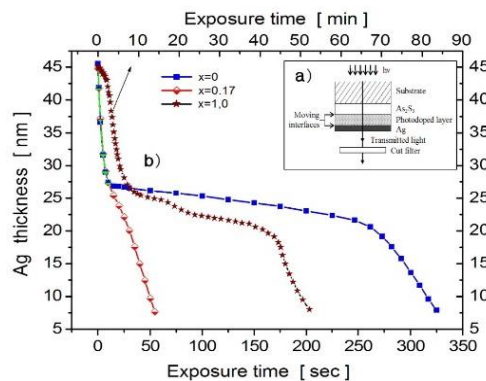


Fig. 1. a) Schematic cross - section through a sample during the photoformation of a solid electrolyte and b) Decrease of Ag film thickness versus exposure time for several compositions of $(\text{GeS}_4)_x(\text{AsS}_3)_{1-x}$ system.

The molecular additive rules have been developed, what allow assessing the molar concentration of different s.u., applying the experimentally measured density of the glassy material. We have applied the additive rules developed by Muller and co-workers for glassy As-S-Ge system [14] to calculate the s.u. molar concentrations for compositions $(\text{GeS}_4)_x(\text{AsS}_3)_{1-x}$, (Table 1), which are the subject of the present investigation. From Table 1 it is seen that the concentration of trigonal s.u. $[\text{AsS}]_{3/2}$ decreases but the concentration of tetrahedral $[\text{GeS}]_{4/2}$ s.u. increases monotonically. At the same time, the concentration of $[\text{S-S}]_{2/2}$ s.u. does not vary essentially, that is all glassy materials in question, comprise nearly the same concentration of free sulphur. The last, leads to overlapping of kinetics curves on the first stage of PD (Fig. 1b) and to a weak variation (except of GeS_4) of the rate of solid electrolyte formation with composition change (Fig.2a).

Farther, the absorption of photons at the doped / undoped chalcogenide interface breaks some of As-S bonds producing the dangling bonds accompanied by generation of free holes, which drifts through superionic region to Ag layer producing the ions by reaction [8,15]:



The Ag^+ ions move in opposite direction i.e. towards the boundary doped / undoped chalcogenide through the superionic region and accepting the electrons from chalcogen dangling bonds lead to creation of ternary superionic Ag-As-S-Ge compound.

The flux of holes (electrons) and Ag^+ ions can be due to both concentration gradient (Fick diffusion) and drift in an electrical field because of a heterojunction formation at the doped / undoped ChG. Thus, this stage of PD depends either on electronic (hole) photoconductivity of doped layer σ_{ph} or its ionic conductivity σ_{Ag^+} .

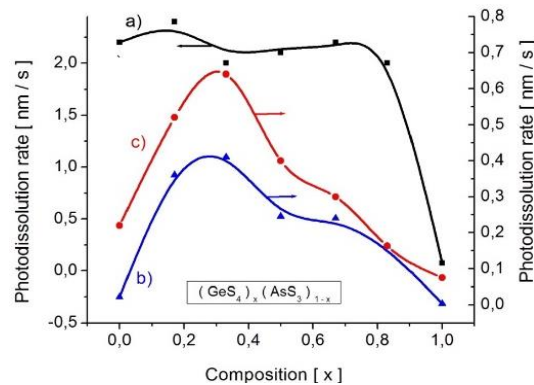


Fig. 2. The photodissolution rate on the first (a), second (b) and third (c) steps versus glass composition.

In our previous paper [7] we have shown that the rate of solid state reaction at the second (II) step of PD process is limited by Ag^+ -ion conductivity under condition that $\sigma_{ph} \gg \sigma_{\text{Ag}^+}$, but the third (III) step is a reaction limited process, controlled by photoconductivity σ_{ph} under condition that $\sigma_{ph} \ll \sigma_{\text{Ag}^+}$. That is why; at this stage the PD kinetics (Fig. 1) exhibits two linear dependencies (steps) of the change of Ag thickness on time that means the constant rates of solid electrolyte formation. It is interesting that the slopes of these linear dependencies that are the rates of reaction strongly depend on the glass composition. Figure 2 (b and c) shows the PD rate of Ag layer (photoformation of solid electrolyte) versus composition of the glassy backbone, for both second (II) and third (III) steps of the solid state reaction. It is seen that in both cases the rate of

solid electrolyte photoformation exhibits a maximum around $(\text{GeS}_4)_{0.33}(\text{AsS}_3)_{0.67}$. In this respect, we have tested the flowing of DC through the fabricated solid electrolytes, at room temperature. The results are given on Figure 3 that shows the electrical resistance of the solid electrolyte versus composition of the glassy backbone. It is seen that the solid electrolytes based on glasses with composition around $(\text{GeS}_4)_{0.33}(\text{AsS}_3)_{0.67}$ exhibit the minimal electrical resistance, that is they are the most conductive. These results indicate that both the process of photoformation of solid electrolytes and their electrical properties depend on the glassy backbone.

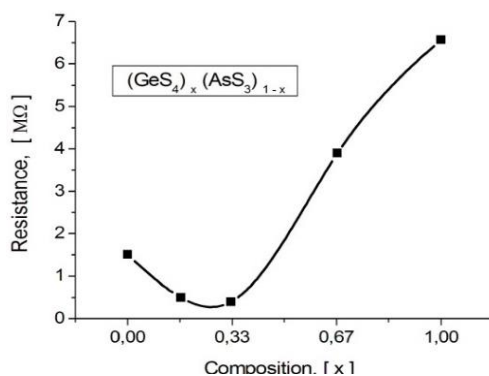


Fig. 3. The electrical resistance of solid electrolytes Ag: $\text{GeS}_4 - \text{AsS}_3$ versus composition of glassy backbone.

To obtain information about the backbone structure of the glassy materials used in this work, we have studied their optical transmission spectra in the far-infrared region. The results are shown in Figure 4 together with IR spectra of glass As_2S_3 and GeS_2 .

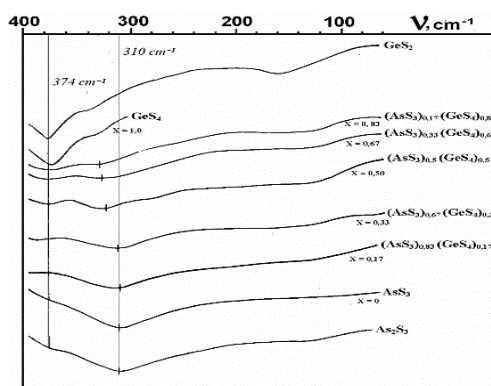


Fig 4. Far infrared transmission spectra of As_2S_3 , GeS_2 and ternary $(\text{GeS}_4)_x(\text{AsS}_3)_{1-x}$.

It is seen that both As_2S_3 and AsS_3 exhibits an oscillatory mode at 310 cm^{-1} that corresponds to A - S bonds. Introduction into the melt of about 8 at.% of Ge, that is composition $(\text{GeS}_4)_{0.33}(\text{AsS}_3)_{0.67}$, leads to the appearance of an additional absorption band in the region of 374 cm^{-1} , which is typical for Ge-S bonds in GeS_2 . Increasing of the Ge content, results in increasing of the high - frequency mode intensity, but the low-frequency mode intensity decreases, so that in GeS_4 only the high-frequency mode at 374 cm^{-1} can be observed. We assume that the maxima of both rates of solid electrolyte photoformation at the second (II) and third (III) steps of PD, as well as the minimum of the electrical resistance around composition $(\text{GeS}_4)_{0.33}(\text{AsS}_3)_{0.67}$ are due to change in the morphology of material i.e. to homogenization of the glassy backbone.

A homogeneous backbone promotes the transport of both electrons and ions involved in photoreaction and in electrical conductivity of the fabricated solid electrolyte, because of lack of phase boundaries and additional defects.

4. Conclusions

The glassy As-S-Ge alloys can be successfully used for fabrication of solid electrolytes via photodissolution of Ag. The process of photoformation and electrical properties of quaternary Ag: GeS₄ - AsS₃ solid electrolytes strongly depend on composition and structure of glassy backbone, showing the best performance for the alloy comprising about 8 at.% Ge.

Acknowledgements

This work was financially supported by Technical University of Moldova through Institutional Grant 15.817.02.29A.

References

- [1] M. N. Kozicki, M. Mitkova, US Patent No.: US 6,998,312 B2 (2006)
- [2] M. N. Kozicki, N.E. Gilbert, C. Gopalan, M. Balakrishnan, C. Ratnakumar, M. Mitkova, Proc. Intern. Conf. on Electronic Devices and Memory, Grenoble, 2005, p. 48.
- [3] E. Bychkov, Yu. Tveryanovich, Yu. Vlasov, Semiconductors and Semimetals **80**, 103 (2004).
- [4] J. Plochanski, J. Przulski, M. Teodorczyk, J. Non - Crystalline Solids **93**, 303 (1987).
- [5] M. T. Kostyshin, F. U. Mikhailovskya, P. F. Romanenko, Sov.Phys. Solid State **8**,451 (1966).
- [6] J. M. Oldale, S. R. Eliot, J. Non - Crystalline Solids **128**, 255 (1991).
- [7] D. Tsiulyanu, I. Stratan, J. Non - Crystalline Solids **356**, 147 (2010).
- [8] S. R. Elliott, J. Non-Cryst. Solids **130**, 85 (1991).
- [9] M. N. Kozicki, M. Mitkova, J. P.Aberouette, Physica E. **19**, 61 (2003).
- [10] I. Stratan, D. Tsiulyanu, I. Eisele, J. Optoelectr. Adv. M. **8**, 2117 (2006).
- [11] X. Sun, R. Hong, H. Hou, Z. Fan, J. Shao, Thin Solid Films **515**, 6962 (2007).
- [12] H. Jain, A. Kovalskiy, A. Miller, J. Non - Crystalline. Solids **352**, 562 (2006).
- [13] R. L. Myuller, in: Solid State Chemistry, edited by Z.U. Borisova, (Consultants Bureau), New York, 1966), p. 1.
- [14] R. L. Myuller, G. M.Orlova, V. N. Timofeeva, G. I. Ternovaia, Vestnik Leningrad. Univ, Seriya Fiz. i Khim. **22**, 146 (1962) (in Russian).
- [15] A. V. Kolobov, S. R. Elliott, M. A. Taguirdzhanov, Philos. Mag. B **61**, 859 (1990).